New generation projection optics for ArF lithography

Yuji Chiba and Kazuhiro Takahashi
Canon Inc.
23-10, Kiyohara-Kogyo-Danchi, Utsunomiya-shi, Tochigi-ken, 321-3231, JAPAN

ABSTRACT

We have developed an ArF scanner with 0.7NA, the FPA-5000AS2, to meet the requirements of the semiconductor industry. The biggest improvement of this system from the previous model is its projection optics. The new projection lens design allows residual aberrations to be extremely small in order to satisfy the requirements of increasingly severe device production. Furthermore, the aberrations derived from the manufacturing process are minimized in the same manner as conventional i-line and KrF lenses by precisely measuring them with a phase measuring interferometer (PMI). To reduce manufacturing-induced aberrations, we calculate various components of imaging performance at each lens manufacturing process and feed them back to the tuning process. Focusing only on aberration in the expression of root mean square (RMS) can never be sufficient for optimal aberration reduction. Lens performance can be optimally improved by gaining a balance among Zernike terms, which represent aberrations, for critical dimensions of various device patterns. It helps us supply users with a projection lens having performance that meets their requirements. This paper reports on the imaging performance of the new lens for both static and dynamic exposure as well as simulation results using PMI data. It also presents the mechanical barrel system that holds the high performance projection lens, intrinsic birefringence (IBR) of CaF_2, and leading-edge ArF lens technologies such as chemical clean technology. And imaging performance of the newest 0.75NA ArF projection lens is demonstrated.

1. INTRODUCTION

The expansion of today's information-intensive society would have been impossible without the progress in semiconductor technologies. In particular, the movement to higher density, higher speed semiconductor chips, which has been realized by the semiconductor industry, is a great contributor to the evolution of information technology (IT). The super fine processing technologies, which have been supporting the growing semiconductor industry, achieved a minimum feature size of 1.0 μm for mass production devices in 1982, and now is expected with 100 nm size in 2002. Among these technologies, optical fine processing has consistently played an important role as the mainstream technology and continued to improve since it was developed in 1950s. With this advancement of the fine fabrication technologies, the exposure wavelength of lithography tools has been progressively becoming shorter such as g-line, i-line to KrF and ArF exposure lights. The majority of the state-of-the-art full-scale chip fabrication uses KrF tools at present, with ArF tools expected to replace them as leading player in a few years.

ArF lithography was ordinary expected to come on the stage for 130 nm node, but is being shifted to the 100 nm node and below because of the extension of high NA KrF tools[1] and resolution enhancement techniques (RET) coming into practical use. However, even with high NA KrF tools, k1 factor is becoming smaller due to the shrinkage of linewidth, and process margin is also reduced despite of the use of strong RET. It is therefore desired that ArF tools be introduced to the industry.

This paper presents optical performance of the 0.70 NA projection lens of the FPA-5000AS2 ArF scanner which was developed to meet the accelerating shrinkage of semiconductor device patterns, together with the barrel system that supports the projection lens.

2. DEVELOPMENT TARGET & SPECIFICATION

Figure 1 shows the ITRS 2001 roadmap. It indicates that the introduction of ArF exposure tools would be in the second half of 2001 for the resolution required by beyond 130 nm nodes, and that critical device production employing ArF tools will start in 2002. There is a tendency to begin the application of ArF tools with logic devices such as MPU

Optical Microlithography XV, Anthony Yen, Editor, Proceedings
of SPIE Vol. 4691 (2002) © 2002 SPIE · 0277-786X/02/$15.00

where fine patterning is required. Intensive introduction is expected in 2003 when the half pitch goes down to 100 nm.

The FPA-5000AS2 meets the requirement of introduction timing of ArF lithography and is regarded as a tool used at linewidths (half pitch) ranging from 110 nm to 90 nm. We simulated DOF for this range of linewidths, and the result is shown in Figure 2. The six graphs are for dense patterns with three linewidths, 110 nm, 100 nm, and 90 nm, using binary mask and attenuated phase shift mask (att-PSM). The horizontal axis of each graph is for NA from 0.5 to 0.9, the vertical axis shows illumination sigma. For binary mask and att-PSM, 2/3 annular illumination was used for the simulation with outer sigma varying from 0.6 to 1.0. The dark dote represents the FPA-5000AS2, and the white dote represents the FPA-5000AS3, whose outer sigma is 0.85.

Looking at the DOF with binary mask, we can see over 0.6 μm DOF is secured at 110 nm dense lines. However, the DOF at 100 nm is around 0.4 to 0.5 nm, and at 90 nm, we can hardly gain DOF. It is therefore inevitable to use phase shift masks, either att-PSM or alt-PSM, to realize the linewidth below 100 nm with ArF lithography. Especially with alt-PSM, the peak of DOF shows in the region where the NA is smaller than the Binary case, which consequently makes it possible to obtain enough DOF even at 90 nm.

In summary, we have seen that the FPA-5000AS2 can provide DOF of over 0.6 μm at 110 nm and around 0.5 μm at 100 nm with binary mask and can give enough DOF at 90 nm when PSM is used while achieving required resolution.

3. LENS FABRICATION TECHNOLOGIES

3.1 Optical materials

Optical materials for the ArF generation include amorphous quartz and single-crystal CaF_2. The challenge in optical materials is intrinsic birefringence (IBR) of CaF_2. We have addressed this lens material property emptying a concept of Wavefront Engineering for the ArF generation and beyond. Wavefront Engineering is a scientific method based on Zernike coefficients to quantify projection lens performance from its design phase to assembly, being an idea of lens manufacturing techniques which enables extremely low aberrations[2].

The challenge, IBR of CaF_2, is a property of being inherently birefringent due to the crystal structure depending on the orientation of the crystal[3]. Figure 3 shows the relation between the amount of IBR of CaF_2 and the crystal axes. If lens elements made of CaF_2 having IBR are assembled with no consideration paid to the crystal axis, contrast is lost due to birefringence, resulting in possible significant degradation in imaging performance.

The left graph of Figure 3 shows the size of CaF_2's IBR for each crystal axis. When the direction of the light coming into the lens changes from [001] to [111] and further to [110] crystal axes, the amount of IBR also changes as shown in the graph on the right of Figure 3. We have come up with a phase combining method of the crystal axis for the FPA-5000AS2 with IBR taken into account. In order to verify the effectiveness of the method, we developed a tool for computing the amount of IBR and corresponding wavefront aberration, and calculated optimal combination of CaF_2 crystal orientations using the tool. In this calculation, we set the orientation of all of the CaF_2 elements to be [111] and optimized the rotation of axis, or the lens clocking, of some of the elements. As a result, it was found that contrast loss was as small as 1 to 2% of the ideal lens contrast, which was enabled just with the above conditions, i.e. [111] crystal orientation and partially optimized clocking, otherwise the same as the customary lens element combining process. Figure 4 is an example of simulating wavefront aberration with optimized clocking of lens elements. In this simulation, we assumed a linearly polarized wavefront to come into the lens and the other wavefront coming out of the lens with its polarization same as the incident wavefront. Figure 4 shows the aberration of that wavefront with the corresponding contrast loss. These results demonstrate that the FPA-5000AS2 fully satisfies the required performance even when the crystal orientation of the CaF_2 elements is restricted to [111] axis, just by controlling the clocking of the elements.

In summary, a solution has been found for the FPA-5000AS2 that can subdue the impact of CaF_2's IBR to a negligible level by controlling the clocking of lens elements.

3.2 Lens barrel techn logies

Another key technology bolstering up the optical performance is the projection lens barrel structure. Early in the

optics design phase, we see lenses as structural components, and the influence of lens deformation due to gravity is analyzed and fed back to optical design. Also, in an attempt to reduce deformation of lenses while being held by the barrel, we have established lens barrel design techniques based on Wavefront Engineering in which the impact of deformation on optical performance is quantified by expressing the figure of the lens in the barrel in terms of Zernike coefficients. This section will present the outline of the projection optics system of the FPA-5000AS2 and the new lens driving mechanism for compensating aberrations.

Figure 5 outlines the FPA-5000AS2's projection optics in which three lens driving units are intended for correcting magnification, distortion and image field deviation (IFD) while coma is compensated for by minutely adjusting the wavelength of the ArF laser. The space inside the lens barrel is divided into three segments; the top and the bottom parts are N2-purged while the middle section is He-purged.

Lens drive mechanisms for correcting aberrations are required to be more and more accurate because various aberrations should be controlled using high precision lens drive system in order to assure imaging performance which becomes acceleratingly severer for each generation. The drive system is also required to be compact in height. To enhance the exposure performance by reducing aberrations, especially for low aberration required lens, the number of lens elements tends to increase, making the lens configuration more complicated. Lens drive units need to fit within such a complex configuration and be optimally placed as well.

The upper illustration in Figure 6 shows the basic structure of the new lens drive unit for the FPA-5000AS2. It comprises of an inner barrel to hold the lens element, an outer barrel coaxial with the inner barrel, a parallel pair of torus-shaped flat ring springs which connect the inner and the outer barrels, and clamping parts for pressing and sealing the flat ring springs. As shown in the lower illustration in Figure 6, they are all axisymmetric, and therefore the space surrounded by them is hermetically closed which forms small chamber. When high-pressure air is applied to the small chamber through a servo valve, there will be a change in the volume of air due to pressure change. This volume will be then converted into the change in the relative vertical position of the outer and the inner barrels. The lens position is thus controlled using a high accuracy displacement sensor. This configuration enabled the whole drive unit to be more compact than that for the previous driving mechanism.

With the adoption of the new compact lens drive unit for correcting aberrations, more flexible placement has been possible, and consequently the projection lens could be optimally designed to minimize aberrations which may be induce by this dive mechanism.

3.3 Chemical clean technologies

Chemical clean technologies are key to ArF lithography more than ever as it can alleviate the "contamination" of lenses. Lens contamination occurs due to photochemical reactions as shown in Figure 7. It is an immediate cause of transmittance deterioration that damages throughput. With ArF wavelength, as it is shorter than KrF, photolytic reactions are more likely to occur for suspended substances in the exposure path because of higher energy of ArF wavelength. In addition, it is known that the influence of deposited substances on lens transmittance is larger than KrF.

Figure 8 illustrates the purged portion for the FPA-5000AS2 exposure system. The purging concept shown in Figure 8 is almost insensitive to clean room or chamber environment because only a few optical surfaces are unpurged. Inside the purged area, cleanliness enough to prevent deposition is maintained by adopting the cleaning process optimized through a variety of experiments and by choosing materials based on their cleanliness.

Figure 9 plots transmittance changes of lenses for ArF and KrF light sources in the storage environment. Three types of samples were prepared for each wavelength for the experiment: SiO_2, CaF_2, and CaF_2 with anti-reflection coating. The samples were left in the clean room for a long period of time, and it was observed that a minute amount of organic gases in the environment was deposited onto the lens surface. The effect of deposition is significant for ArF, implying that transmittance can deteriorate depending on the environment even where no photochemical reactions occur.

Consequently, ArF lithography tools need to be manufactured in a chemically clean environment all through the manufacturing processes from optical and mechanical parts processing to total integration of modules. Our chemical

clean technologies have been established through experiment-based quantitative evaluations. For the exposure system of FPA-5000AS2, the total amount of organic gases at the gas exit of the purged area is reduced down to a couple of $\mu g/m^3$ in terms of toluene volume, which is almost the same level as the input gas to the purged area. As a result, lens contamination of the FPA-5000AS2 is minimized and chemical cleanliness is maintained.

4. LENS PERFORMANCE

4.1 Aberration level

In this chapter, the aberration of the FPA-5000AS2 projection optics as it lens alone is presented. Wavefront aberrations are measured at multiple image heights within the exposure slit by PMI which uses the wavelength same as the exposure tool, i.e. 193 nm. The desired optical performance is achieved by applying Wavefront Engineering with Zernike coefficients, and by adding some adjustment processes as well[2]. Normally, the aberration of a lens is described in RMS of 36 Zernike terms. The RMS values of the latest five projection lens are shown in Figure 10, which shows the maximum values within the slit. It also shows the average RMS of the projection lenses of FPA-5000ES3 KrF scanners with 0.73 NA for reference. The aberrations of the ArF lenses are equal to or smaller than the latest volume production KrF scanner, indicating that the FPA-5000AS2 enables low aberrations required for low-k1 lithography.

In addition to the requirement of small RMS, well-balanced adjustment of aberrations is necessary to meet the 100 nm node demands. For example, capacitor patterns consisting of a pair of honeycomb contact holes and active area patterns of DRAM devices are sensitive to aberrations[1,4]. These patterns are especially sensitive to asymmetric aberrations such as 3? and 1?. By calculating sensitivity of these patterns to each Zernike coefficient, printed asymmetry of these patterns can be easily characterized from wavefront aberration data measured with PMI. As an example of 1? and 3?, CD difference between both ends of a five bar pattern and size difference between a pair of holes for a capacitor pattern are shown, respectively, in Figure 11 for the latest five lenses. It shows good symmetry in the printed device patterns, which resulted from the balancing of aberrations.

Figures 12 and 13 shows IFD and distortion of the latest five lenses, respectively. IFD is calculated as the range of best focus positions of vertical and horizontal patterns measured with PMI at multiple points in the slit, while distortion is obtained as a result of exposure on a Test Bench. Both figures represent the lens-related components, which are averaged in the scan direction. Below 65 nm IFD and below 8 nm distortion have been achieved.

4.2 Imaging performance

This section reports on the optical performance of scanning exposure with the FPA-5000AS2. Figure 14 shows CD characteristics of 110 nm L&S at 13 points in a 26 mm x 33 mm field. The NA was 0.70, with 2/3 annular illumination with outer sigma 0.85. A binary mask was used. Sumitomo PAR-718 resist was coated with a thickness of 3000A over a BARC of AR19 with a thickness of 820A. Common DOF of the L&S pattern is 0.45 μm and CD uniformity at the best focus is 6 nm.

Figure 15 shows IFD and astigmatism of scanning exposure. The best focus for a vertical and horizontal pattern chart at each field point is determined by quartic approximation of SEM measurements of CD focus characteristics of an isolated 110 nm line. Figure 15 represent lens-related component, and IFD within the slit is 55 nm while the maximum astigmatism is 41 nm. The IFD over the full 26 mm x 33 mm field is 60 nm.

Figure 16 is the result of dynamic distortion during scanning. The residual distortion is DX=6.6nm and DY=7.2nm.

Figure 17 is SEM cross-sections of 100 nm 1:1 dense patterns. DOF of 0.6 μm for 100 nm is acquired at 0.70 NA with 2/3 annular illumination using a binary mask. Other process conditions are the same as Figure 14. Figure 18 is SEM cross-sections which show the resolution limit of dynamic exposure for L&S patterns. FUJIFILM-Arch GAR-8105G1 resist was coated with a thickness of 3000A over a BARC of AR19 with a thickness of 820A, with TARC of Clariant AZ-AQUATAR-VI-A30 with a thickness of 330A. Resolution limit of 950A is obtained using a binary mask.

Figure 19 is SEM pictures which shows the resolution limit for 1:1 dense contact holes with dynamic exposure. NA

was 0.70 with 0.85 sigma and an att-PSM was used with a transmittance of 6%. Sumitomo AX-5186A35 resist was coated with a thickness of 4250A over a BARC of Brewer Science AEC-29-8 with a thickness of 780A, with TARC of AZ-AQUATAR-VI-A30 with a thickness of 330A. Resolution limit of 110 nm is achieved for 1:1 dense contact holes.

Figure 20 shows the imaging performance of the newest 0.75 NA projection lens of the FPA-5000AS3 ArF scanner. These SEM cross-sections photograph show 90nm dense patterns DOF and resolution limit exposed on Test Bench. DOF of 0.4 μm for 90 nm is achieved at 0.75 NA with 2/3 annular illumination using an att-PSM with transmittance of 6%. TOK TarF-6a-101 resist was coated with a thickness of 2700A over an organic BARC with a thickness of 820A. Resolution limit of 85 nm with 0.2μm DOF is obtained using an att-PSM.

5. CONCLUSION

We have implemented new concept technologies to the manufacturing of leading-edge ArF lithography lenses for the 110 nm node and beyond. A lens development tool was built with IBR of CaF_2 enabling production of extremely low aberration lenses. For the barrel that mechanically holds the lens, we have developed a new purging system and a new lens drive unit, both of which are another contributor to achieving extremely low aberrations. In addition, by realizing ultimate chemical clean technologies, long-term assurance of lens performance to avoid contamination has been made possible. IFD and distortion of the FPA-5000AS2 ArF scanner designed for the 100 nm node have been also demonstrated. And a result of exposure of FPA-5000AS3 NA0.75 showed the possibility of the mass production beyond 100nm node.

ACKNOWLEDGEMENTS

The authors wish to thank Masakatsu Ohta for his advice and encouragement throughout this work. We also wish to thank Ikuko Miura for her help in writing this paper. Finally we acknowledge our colleagues for their contributions to simulations and data collections.

REFERENCES

1. T. Kanda et al., "New-generation projection optics for microlithography," SPIE 2001, Vol. 4346, pp595-605
2. T. Yoshihara et al., "Realization of very-small aberration projection lenses," SPIE 2000, Vol.4000 pp559-566
3. J. Burnett et al., "Intrinsic Birefringence in 157 nm Materials," The SEMATECH Calcium Fluoride Birefringence Workshop, 18 July, 2001, San Francisco, CA
4. J. Finders et al., "Can DUV take us below 100nm?", SPIE 2001, Vol. 4346, pp153-165

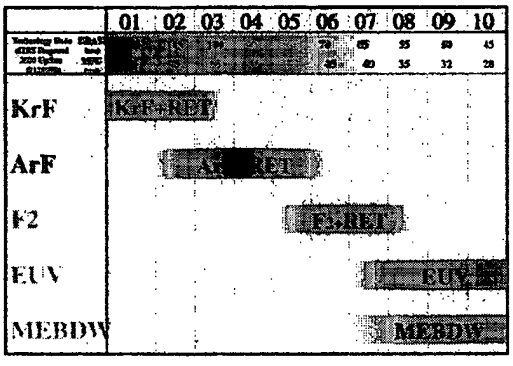

Fig.1 Optical Lithography Roadmap

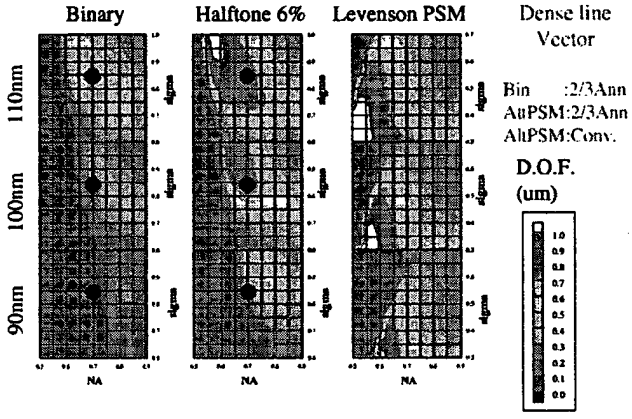

Fig.2 NA/sigma Optimization for ArF (Contrast 40% DOF)

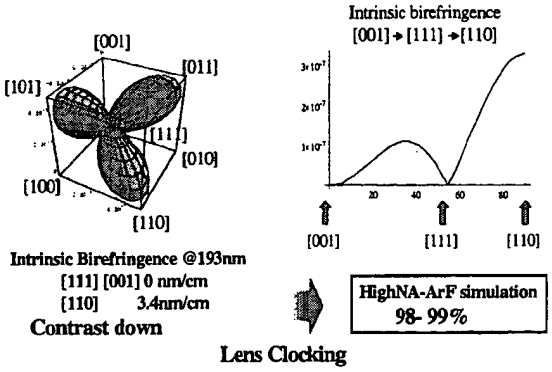

Fig.3 Influence of Intrinsic Birefringence

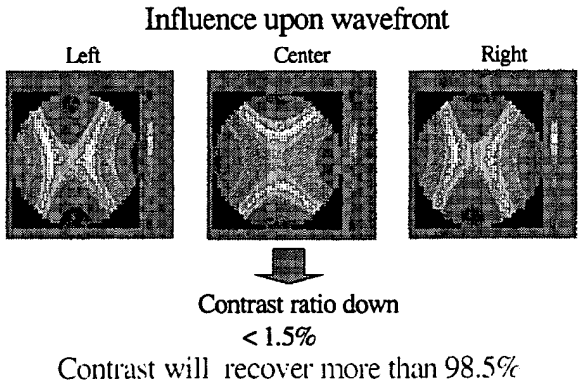

Fig.4 Solution for IBR

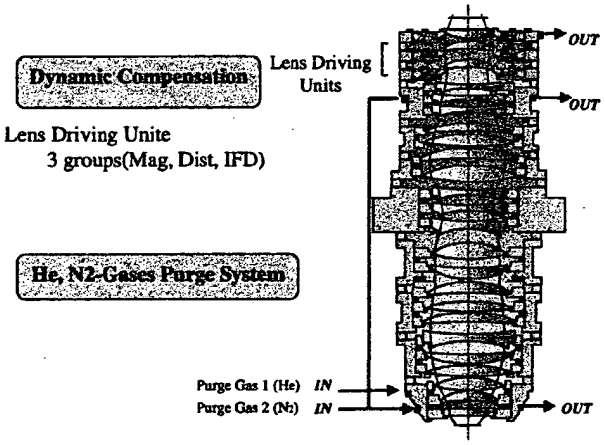

Fig.5 Projection Lens System Features

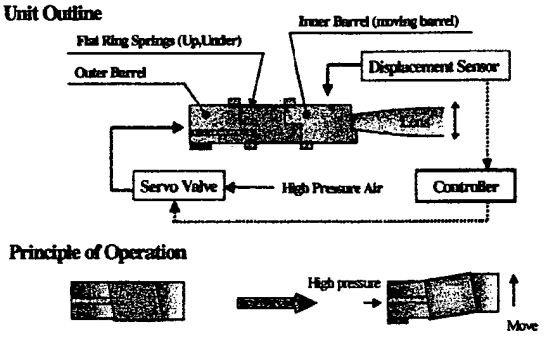

Fig.6 New Concept Lens Driving Unite

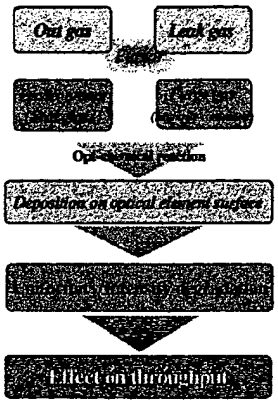

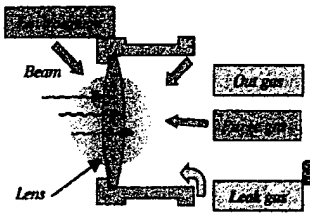

Fig.7 Influence upon optics

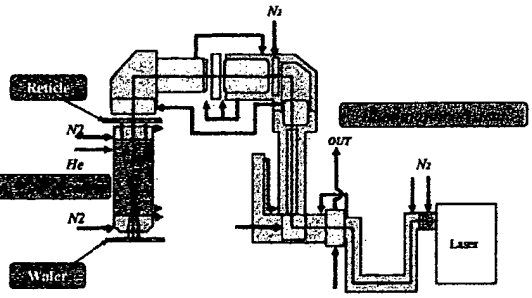

FPA-5000AS2 Exposure's purge system schematic

Fig.8 Purge System for Exposure Area

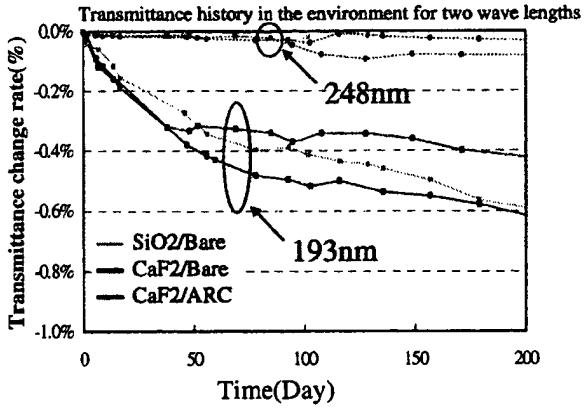

Fig.9 Requirement of chemical contamination for storage and assembly environment after ArF

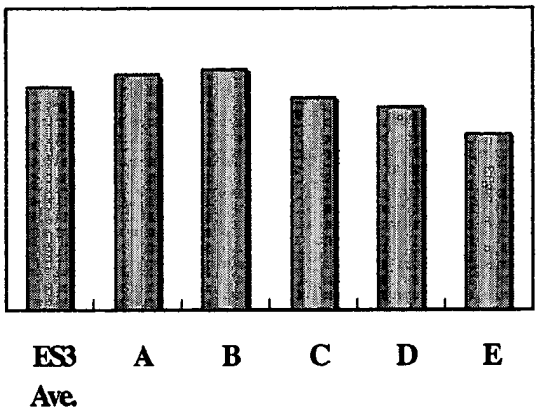

Fig.10 RMS Comparison AS2 vs. ES3

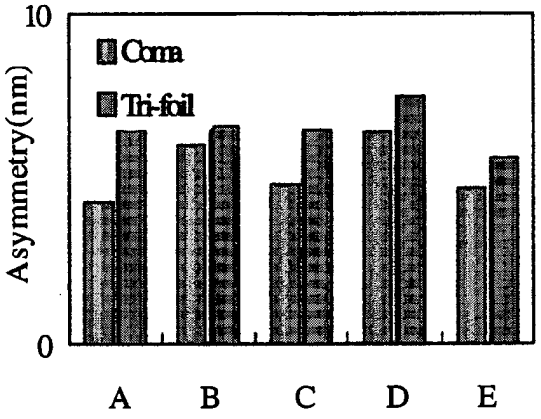

Fig .11 Coma &3? simulated results

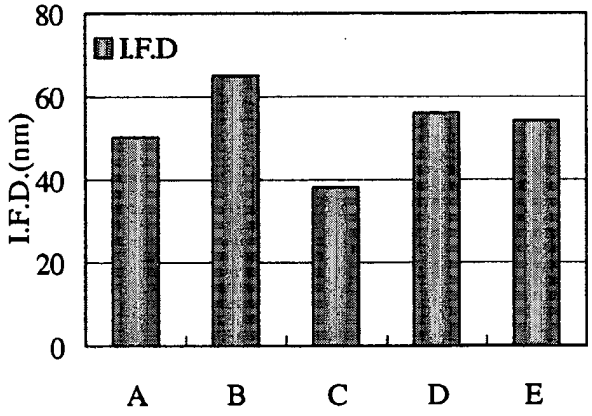

Fig.12 IFD simulated results by PMI

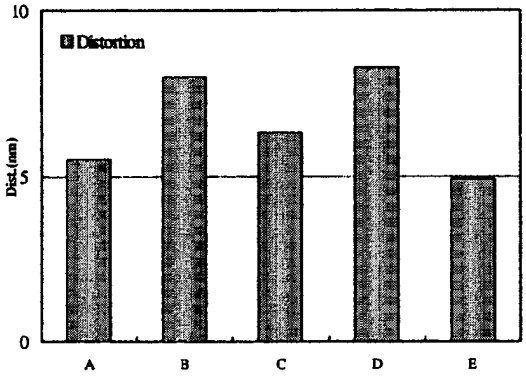

Fig.13 Distortion espoused by Test bench (scan direction average)

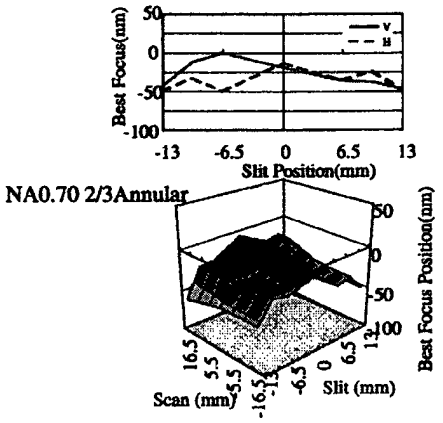

Fig14. Dynamic Image Field Deviation

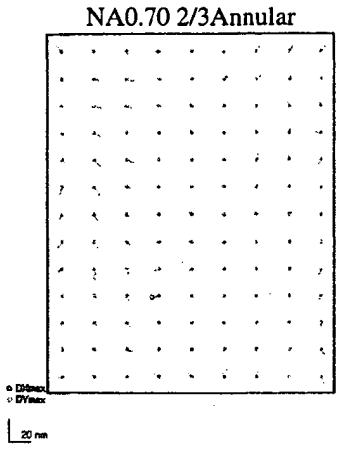

Fig15. Dynamic Distortion

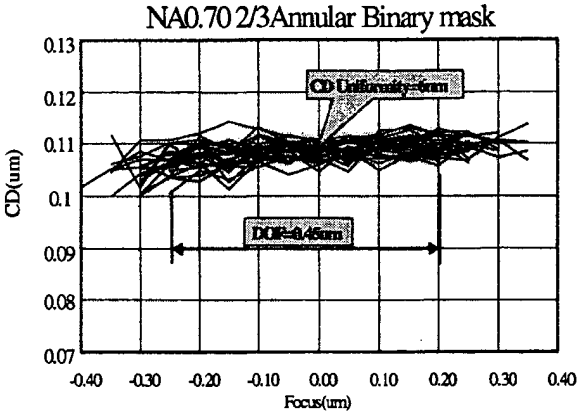

Fig.t16 110nm Lines and Space Pattern CD DOF & Uniformity (Dynamic exposure)

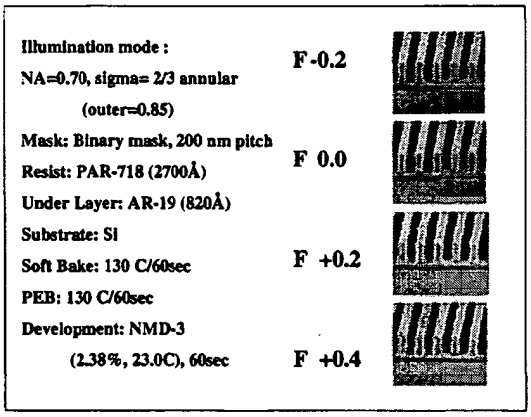

Fig.17 100nm Line & Space Pattern DOF

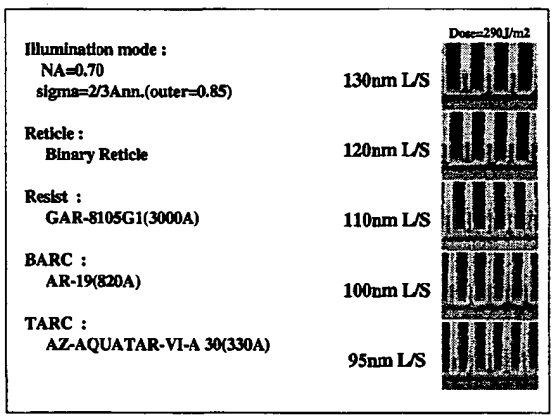

Fig.18 Resist Performance Line &

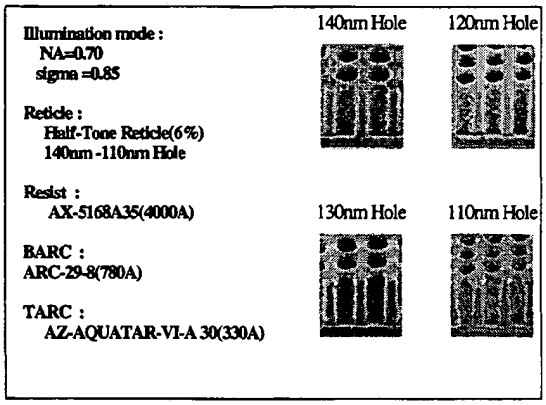

Fig.19 Resist Performance Contact-Hole

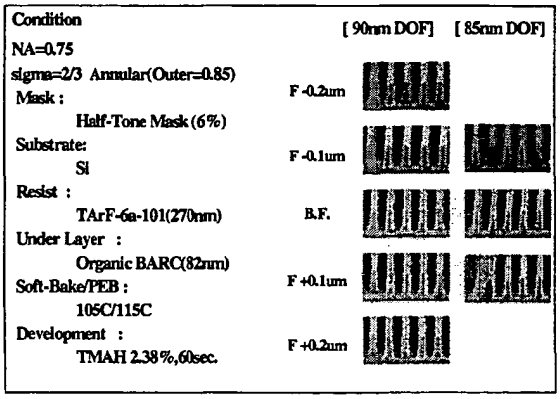

Fig.20 90nm & 85nm Line & Space Pattern DOF